

Article

# Visible-Light-Driven, Dye-Sensitized TiO<sub>2</sub> Photo-Catalyst for Self-Cleaning Cotton Fabrics

Ishaq Ahmad and Chi-wai Kan \*

Institute of Textiles and Clothing, The Hong Kong Polytechnic University, Kowloon, Hong Kong, China; ahmadrai621@gmail.com

\* Correspondence: tccwk@polyu.edu.hk; Tel.: +852-2766-6531

Academic Editor: Silvia Gross

Received: 28 July 2017; Accepted: 3 November 2017; Published: 6 November 2017

**Abstract:** We report here the photo-catalytic properties of dye-sensitized TiO<sub>2</sub>-coated cotton fabrics. In this study, visible-light-driven, self-cleaning cotton fabrics were developed by coating the cotton fabrics with dye-sensitized TiO<sub>2</sub>. TiO<sub>2</sub> nano-sol was prepared via the sol-gel method and the cotton fabric was coated with this nano-sol by the dip-pad-dry-cure method. In order to enhance the photo-catalytic properties of this TiO<sub>2</sub>-coated cotton fabric under visible light irradiation, the TiO<sub>2</sub>-coated cotton fabric was dyed with a phthalocyanine-based reactive dye, C.I. Reactive Blue 25 (RB-25), as a dye sensitizer for TiO<sub>2</sub>. The photo-catalytic self-cleaning efficiency of the resulting dye/TiO<sub>2</sub>-coated cotton fabrics was evaluated by degradation of Rhodamine B (RhB) and color co-ordinate measurements. Dye/TiO<sub>2</sub>-coated cotton fabrics show very good photo-catalytic properties under visible light.

**Keywords:** self-cleaning; TiO<sub>2</sub>; visible light active photo-catalyst; dye sensitization; sol-gel method

## 1. Introduction

In the last century, the textile and clothing industries have gained revolutionary developments in many aspects. Advanced scientific research has improved the processing methodology of natural fibers as well as the finishing technology for textile products. Tremendous improvements in the physical and/or chemical treatment of textile surfaces and the development of new functional materials for the finishing of textile products have led to the new textile materials. These multifunctional products have a wide variety of applications in many fields, including health, safety and protection, medical and hygiene, clothing, construction, agriculture, transport, electronics, geo-textiles and packaging [1]. Cotton and some of the synthetic polymers are mostly used as raw materials for the textiles. However, cotton has many advantages over synthetic polymers due to its softness, breathability, biodegradability, high performance and environmentally-friendly nature [2]. Raw cotton is converted into fibers which are further processed into cotton fabrics either by a weaving or knitting process. The resulting cotton fabrics are subjected to a variety of finishing processes according to the end-product requirements. Finishing processes may be divided into two major steps i.e., (1) physical and/or chemical pretreatment of the surface of the cotton fabrics; (2) application of dyes or other functional materials to the cotton fabrics to get the final products. In the last few decades, surface pretreatment and nano-functionalization of cotton fabrics for multiple applications has been a major focus for researchers. The development of self-cleaning textile fabrics using finishing processes is one of the promising research areas in textile technology.

Self-cleaning is one of the most fascinating natural phenomena, which was observed in lotus plant leaves for the first time, and now many superhydrophobic and self-cleaning surfaces have been developed using this phenomenon [2,3]. In general, a self-cleaning surface has the ability to maintain a clean and contamination-free surface either by avoiding the deposition of dust and other pollutants or by decomposing the adsorbed stains and contaminants on the surface. In the former process,

the surface is physically and/or chemically treated to develop superomniphobicity, the ability to resist the adsorption of every kind of liquid or other pollutant, to make it dust and pollutant repellent, while in latter case, some photo-active compounds are adsorbed on the surface which decompose the stains and contaminants coming into contact with the surface when exposed to sunlight.

Self-cleaning textile fabrics have been developed by adsorbing photo-active materials on the textile surface. These photo-active materials include  $\text{BiVO}_4$  [4],  $\text{Fe}_2\text{O}_3$  [5],  $\text{ZnO}$  [6],  $\text{WO}_3$  [7] and  $\text{TiO}_2$  [8]. Among these diverse photo-catalysts, nano-crystalline  $\text{TiO}_2$  has been preferentially applied because of its photo-stability, high oxidative power, low cost and non-toxicity [9–11]. Moreover, a transparent, crystalline and stable coating of  $\text{TiO}_2$  nano-particles on the textile fabrics has been easily formed by the sol-gel method [8,10]. The anatase ( $\text{TiO}_2$ )-coated cotton fabric shows remarkable photo-catalytic effects for contaminants, microorganisms and dirt, when exposed to ultraviolet light. However, photo-catalytic applications of anatase have been restricted in the ultraviolet range (only 3–5% of the solar spectrum) due to its wide band gap of 3.2 eV and rapid electron-hole recombination. In addition, weak interaction of the  $\text{TiO}_2$  with textile materials also decreases its practical applications. To increase the attachment of  $\text{TiO}_2$  to textile materials, pretreatment (physical and/or chemical) of the fabrics has been reported [12–14]. Due to the increasing demand for self-cleaning textile products in daily life, visible-light-active  $\text{TiO}_2$  coatings are prerequisites for scalable applications of self-cleaning textiles. Visible-light-driven, self-cleaning textiles have been produced by doping  $\text{TiO}_2$  with metals, non-metals or by mixing with other semiconductor metal oxides. Nano-coatings of N- $\text{TiO}_2$  [15], Au/ $\text{TiO}_2$  [16], Ag/ $\text{TiO}_2$  [17], Pt/ $\text{TiO}_2$  [18], SiO<sub>2</sub>/ $\text{TiO}_2$  [19] have been applied to the cotton and wool fabrics to get visible-light-driven photo-activity for dirt/stain degradation. Although the electron-hole recombination process has been retarded by the substitution of metal ions in  $\text{TiO}_2$  nano-crystals, their optical absorption and photo-catalytic activity in the range of visible light are not satisfactory. Dye photo-sensitization of  $\text{TiO}_2$  nano-particles is another approach to enhance its visible-light-harvesting power. Porphyrin is a synthetic dye, a structural analogue of chlorophyll, with spectral absorption in the near-visible region. Porphyrin and metal-porphyrin derivatives have been applied to  $\text{TiO}_2$ -coated cotton fabric by post-treatment [20–23]. Porphyrin- $\text{TiO}_2$ -coated cotton fabrics exhibit self-cleaning properties under a narrow range of visible light by degrading the dirt/stains; however, its light absorption is only in a narrow range of the ultraviolet or near-visible light spectrum which reduces its photo-activity. Furthermore, the synthesis process of porphyrin is very complicated and costly, which reduces its practical applications on a large scale. Therefore, there is a need for research to develop durable visible-light-driven, self-cleaning textile fabrics to make fruitful use of sunlight for energy harvesting and for practical applications of the textile cotton fabrics.

Phthalocyanine (PC) is a structural analogue of porphyrin, however, its synthesis process is easy and cost effective. The basic PC structure is given in Figure 1. PC-reactive blue dyes have already been used in the dyeing of textile products. Monomeric metallic PC has characteristic absorption spectra with a Soret band at approximately 350 nm, a small band at 600 nm and a strong absorption peak (Q-band) around 670 nm, with a molar extinction co-efficient of  $10^5 \text{ M}^{-1} \cdot \text{cm}^{-1}$  [24]. This spectral absorption varies by substituting the PC with a variety of substituents at peripheral and non-peripheral positions [25]. Due to its high thermal and chemical stability, relatively stable triplet excited state, high quantum yield of singlet oxygen, good optical properties and low toxicity, PC compounds have been used as photo-sensitizers as well as photo-catalysts for the degradation of environmentally hazardous compounds such as chlorophenols [26–28]. In this study, a (PC) reactive dye (RB-25) was used for the photo-sensitization of  $\text{TiO}_2$  for the development of self-cleaning cotton fabrics.

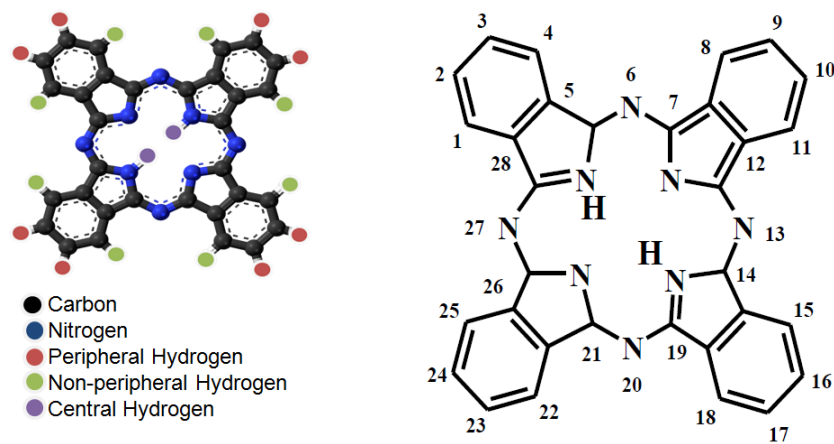


Figure 1. Structure of phthalocyanine.

## 2. Materials and Methods

### 2.1. Materials

This study used 100% scoured and bleached plain woven cotton fabric. The specifications of the cotton fabric used are given in the Table 1.  $\text{TiO}_2$  precursor, titanium tetraisopropoxide (TTIP), glacial acetic acid, absolute ethanol and nitric acid were used as received from the suppliers to prepare  $\text{TiO}_2$  nano-sol. RB-25 dye commercial product was used as a photo-sensitizer as received without further purification. The RB-25 dye structure is given in the Figure 2.

Table 1. The cotton fabric specifications.

Fabric Weight	Yarn Count		Fabric Density	
	Warp	Weft	End/cm	Picks/cm
119 g/m <sup>2</sup>	40	40	52	28

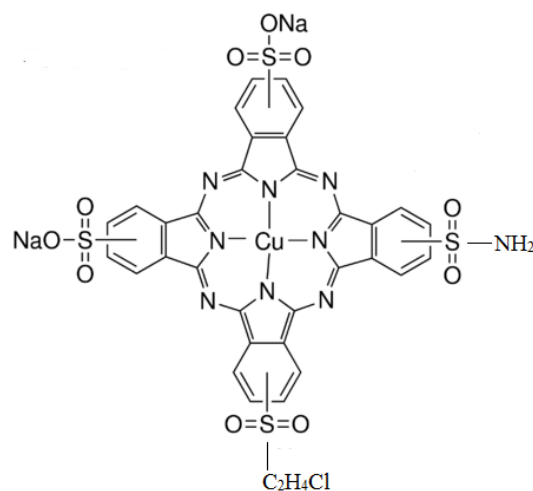


Figure 2. Chemical structure of RB-25.

### 2.2. Preparation of $\text{TiO}_2$ Nano-Sol

A total of 10 mL of TTIP was dissolved in 50 mL of absolute ethanol. The TTIP solution was added dropwise to the acidified water-ethanol (5:1) mixture with a pH of 5. The mixture was stirred at 70 °C for 16 h.

### 2.3. Coating of Cotton Fabric with TiO Nano-Sol

The cotton fabric was completely washed and dried under standard atmospheric conditions before the coating process. The prepared TiO<sub>2</sub> nano-sol was coated on the cotton fabric by dip-pad-dry-cure method. In detail, the cleaned cotton fabric was dipped in the TiO<sub>2</sub> nano-sol for 5 min, and pressed with a padder machine (Rapid Labortex Co., Ltd., Taipei, Taiwan). The nip pressure was kept at 2.5 kg·cm<sup>-2</sup> to assure the same coating amount of TiO<sub>2</sub> on each of the cotton fabric samples. The wet pick up of TiO<sub>2</sub> sol was about 77%. The padded fabrics were neutralized to pH 7 by conventional spraying with aqueous solution of Na<sub>2</sub>CO<sub>3</sub>. The TiO<sub>2</sub>-coated cotton fabric samples were dried in a preheated oven at 80 °C for 5 min and finally cured at 120 °C in a preheated curing machine (Mathis Labdryer Labor-Trockner Type LTE, Werner Mathis AG Co., Oberhasli, Switzerland) for 3 min.

### 2.4. Dyeing of the TiO<sub>2</sub>-Coated Cotton Fabric

The TiO<sub>2</sub>-coated cotton fabrics were dipped in dye solutions of RB-25 with different dye concentrations of 0.01, 0.016, 0.08 and 0.16 mg/L for 2 h at 70 °C in a dyeing bath. The resulting dyed fabrics were first washed with hot water and then with de-ionized water to remove the unattached TiO<sub>2</sub> and dye molecules. The samples were dried for further characterization.

### 2.5. Staining of the Dye/TiO<sub>2</sub>-Coated Cotton Fabrics

For self-cleaning studies, 200 µL of aqueous solution of Rhodamine B (RhB) (7.5 mg/L) was applied to each of the TiO<sub>2</sub>/dye-coated cotton fabric samples. The samples were placed on smooth plastic sheets in the dark to avoid the leakage of the stain liquor. The stains were dried and then the stained fabrics were exposed to light (8 W lamp = 464 lm) for 6 h.

### 2.6. Characterization

#### 2.6.1. Fourier Transform Infrared Spectroscopy

The attachment of TiO<sub>2</sub> nano-particles on the cotton fabric was observed by the surface chemical analysis of the samples by a Fourier transform infrared (FTIR) spectrophotometer equipped with an attenuated total reflection (ATR) accessory (Spectrum 100, Perkin Elmer Ltd., Waltham, MA, USA). The FTIR-ATR spectra of pure cotton fabric, TiO<sub>2</sub>-coated and TiO<sub>2</sub>/dye-coated cotton fabrics were obtained in the scanning range of 650–4000 cm<sup>-1</sup> with an average of 64 scans of each fabric.

#### 2.6.2. Photo-Catalytic Degradation of RhB

The self-cleaning performance of the TiO<sub>2</sub>-coated and dye/TiO<sub>2</sub>-coated fabrics was evaluated by the photo-catalytic degradation of RhB according to procedure reported in [8]. The decomposition of RhB was assessed by measuring the decrease in its concentration during the exposure to visible light irradiation. In detail, 3 g of each of the cotton fabric samples was cut into pieces of 1 cm × 1 cm dimensions. These pieces were soaked in 100 mL of the RhB dye aqueous solution (18 mg/L) in a 250 mL glass beaker. The cotton fabric pieces were shaken well in the dye solution and kept in the dark for 1 h to achieve the absorption–desorption equilibrium. The beakers with a test specimen were exposed to visible light under Philip fluorescent lamps with light intensity of 5.2–5.3 mW·cm<sup>-2</sup> on the top of samples while vigorously shaking. A total of 10 mL of the target dye solution was taken out from the beakers after regular time intervals for 6 h and the UV-Visible absorption spectra were recorded on a UV-Visible UH5300 spectrophotometer (Hitachi, Tokyo, Japan). The decrease in the concentration of RhB was estimated by comparison with the concentration of RhB at 555 nm ( $\lambda_{\max}$  of RhB).

### 2.6.3. Color Yield Measurements

The quantitative self-cleaning efficiency of the dye/TiO<sub>2</sub>-coated fabrics was evaluated by color yield by reflectance measured at given wavelength intervals in the visible spectrum by a reflectance spectrophotometer (Macbeth Color-Eye 7000A, X-Rite, Grand Rapids, MI, USA) by using a D65 illuminant and 10° standard observer. The reflectance measurements were taken for each sample three times from 400 to 700 nm with 10 nm intervals.  $K/S$  values were obtained by using the Kubelka-Munk Equation (1) as reported in [29],

$$\frac{K}{S} = \frac{(1 - R)^2}{2R} \quad (1)$$

where  $K$  is the absorption coefficient of the colorant,  $S$  is the scattering coefficient of the colored substrate and  $R$  is the reflectance of the colored sample. The higher the  $K/S$  value, the greater the dye uptake is, resulting in a better color yield.

### 2.6.4. CIE Color Coordinates

The CIE (*Commission Internationale de l'Eclairage* (International Commission on Illumination)) color coordinates, i.e.,  $L^*$  (lightness and darkness),  $a^*$  (redness and greenness) and  $b^*$  (yellowness and blueness) were also obtained by reflectance spectrophotometer (Macbeth Color-Eye 7000A) by using D65 illuminant and 10° standard observer.

### 2.6.5. Surface Morphology

Surface morphologies of the pure cotton fabric, TiO<sub>2</sub> coated cotton fabric and dye/TiO<sub>2</sub> coated cotton fabrics were studied using Scanning Electron Microscope (JSM-6490, JEOL, Tokyo, Japan).

## 3. Results and Discussion

### 3.1. Fourier Transform Infrared Spectroscopy

The FTIR-ATR spectra of the pure cotton fabric, TiO<sub>2</sub>-coated and dye/TiO<sub>2</sub>-coated cotton fabrics are shown in the Figure 3. Figure 3a represents the spectrum of pure cotton fabric. The peaks at around 3289 cm<sup>-1</sup>, 2879 cm<sup>-1</sup>, 1318 cm<sup>-1</sup> and 1038 cm<sup>-1</sup> are associated with the hydroxyl groups (–OH) of cellulose, C–H stretching vibrations of the cellulose chains in the cotton fabrics, C–O, C–H bending vibrations, and C–O, O–H stretching vibrations of the polysaccharide in cellulose respectively [29–31]. The FTIR-ATR spectrum of the TiO<sub>2</sub>-coated cotton fabric is presented in Figure 3b. The decrease in the peak intensity at 3289 cm<sup>-1</sup> and 1038 cm<sup>-1</sup> in Figure 3b indicates the attachment of TiO<sub>2</sub> with the (–OH) group of the cellulose chains on the surface of the cotton fabric. A further decrease in the peak intensity at 3289 cm<sup>-1</sup> in the spectrum of dye/TiO<sub>2</sub> coated cotton fabric, as shown in Figure 3c, indicates the attachment of the dye to the surface of TiO<sub>2</sub>. Furthermore, a relative increase in the peak intensity at 1038 cm<sup>-1</sup> indicates the C–O–C bond formation of the dye molecules with TiO<sub>2</sub>-coated cotton fabric.

### 3.2. UV-Visible Absorption Measurements

In order to study the binding of RB-25 with the TiO<sub>2</sub>-coated cotton fabric, the UV-visible absorption spectra of the RB-25 dye was recorded in the water and on the TiO<sub>2</sub>-coated cotton fabric, as shown in the Figure 4. The UV-visible absorption spectrum of RB-25 in water shows a strong absorption peak (Q-band) at 662 nm. However, this absorption peak (Q-band) was shifted to 676 nm with a red shift of 14 nm. This red shift of 14 nm indicates the strong binding of RB-25 dye with TiO<sub>2</sub>, as reported in a study [20].

The absorption spectrum of the TiO<sub>2</sub>-coated cotton fabric was also recorded, which indicates the formation of an anatase layer on the cotton fabric as shown in the Figure 5.

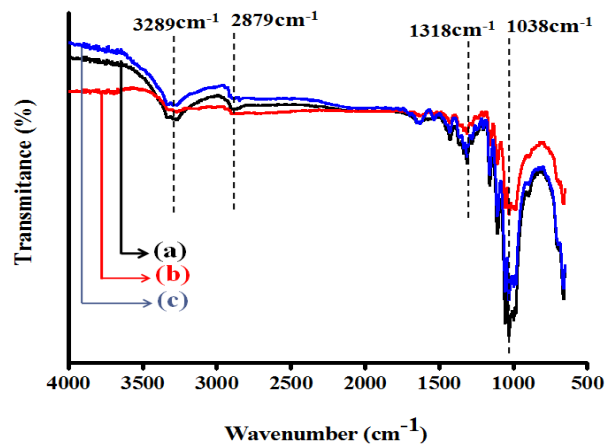


**Figure 3.** FTIR-ATR spectra of cotton fabric: (a) pure cotton fabric; (b) TiO<sub>2</sub> coated cotton fabric; and (c) TiO<sub>2</sub>/dye coated cotton fabric.

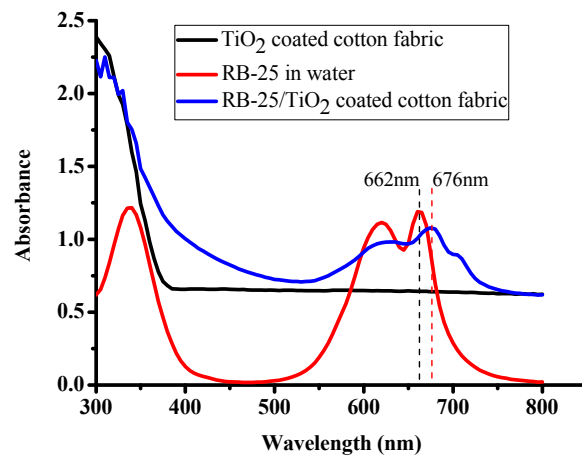


**Figure 4.** UV-Visible absorption spectra of RB-25 in water, TiO<sub>2</sub>-coated cotton fabric and RB-25/TiO<sub>2</sub>-coated cotton fabric.

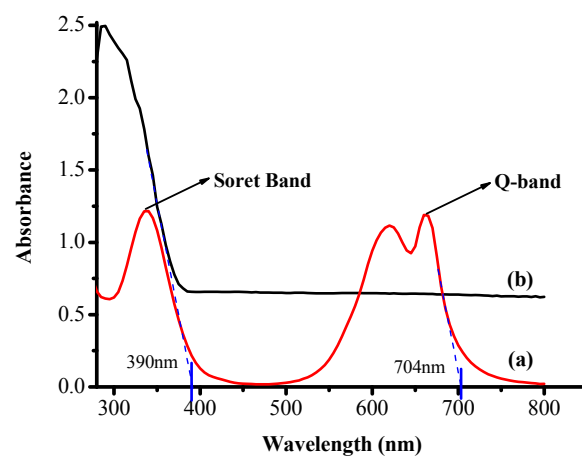


**Figure 5.** UV-Visible absorption spectra of (a) RB-25 in water and (b) TiO<sub>2</sub>-coated cotton fabric.

The energy gaps were measured from the absorption wavelength using a simple energy equation as given in the Table 2.

**Table 2.** Calculations of energy gap.

Sr. No.	Sample	$\lambda$ (m)	Energy (J)	eV
1	TiO <sub>2</sub>	$3.90 \times 10^{-7}$	$5.1 \times 10^{-19}$	3.18
2	RB-25	$7.04 \times 10^{-7}$	$2.82 \times 10^{-19}$	1.76

Band gap energy ( $E$ ) =  $hc/\lambda$   
 $h$  = Planks constant =  $6.626 \times 10^{-34}$  J·s  
 $c$  = speed of light =  $3.0 \times 10^8$  m/s  
 $\lambda$  = cut off absorption wavelength  
Conversion factor: 1 eV =  $1.6 \times 10^{-19}$  J

### 3.3. Photo-Catalytic Degradation of RhB

RhB (C<sub>28</sub>H<sub>31</sub>N<sub>2</sub>O<sub>3</sub>Cl) is a water soluble, basic, red dye. It is widely used as a dye in the textile and clothing industry. It is harmful to human and animal skin, causing irritation to the eyes, skin and respiratory tract. Its severe toxic and carcinogenic effects towards human beings and animals have been reported in the literature [32]. Thus, keeping in view its hazardous effects and red color, it has been used as a target pollutant in this study to evaluate the photo-catalytic efficiency of TiO<sub>2</sub>-coated and dye/TiO<sub>2</sub>-coated cotton fabrics. The decrease in the concentration of RhB by visible light irradiation in the presence of TiO<sub>2</sub>-coated and dye/TiO<sub>2</sub>-coated cotton fabrics was estimated by comparison with the concentration of RhB. The  $C/C_0$  values of the RhB dye solution were plotted against time to observe the degradation rate of RhB, where  $C$  is the concentration of the target dye solution at regular intervals of irradiation calculated from the absorbance spectra, and  $C_0$  is the initial concentration of the dye solution.

The degradation curves of the RhB for TiO<sub>2</sub>-coated and dye/TiO<sub>2</sub>-coated cotton fabrics are compared in Figure 6. RhB was relatively stable under visible light when only TiO<sub>2</sub> was used for the coating of the cotton fabric, as shown in the Figure 6b. However, when the RB-25 dye is adsorbed on the TiO<sub>2</sub>-coated cotton fabric, the RhB undergoes degradation at a different rate, depending on the concentration of the RB-25 used. It can be noted from the degradation curves c, d, e and f in Figure 6 that the degradation rate of RhB increases with a decrease in the RB-25 dye concentration. The reason for the lower degradation rate of RhB at higher concentrations of sensitizer can be attributed to the agglomeration of the sensitizer molecules on the active sites of TiO<sub>2</sub>. When the concentration of the sensitizer was reduced to 0.01 mg/L, the degradation rate increased significantly, indicating that a single layer of sensitizer on the TiO<sub>2</sub> surface is more efficient.

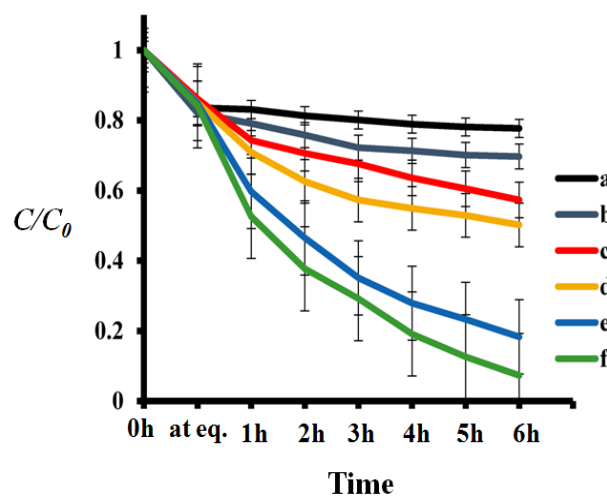


**Figure 6.** The degradation of the RhB for TiO<sub>2</sub>-coated and dye/TiO<sub>2</sub>-coated cotton fabrics: (a) Control dye solution; (b) TiO<sub>2</sub>-coated cotton fabric. While (c), (d), (e) and (f) are dye/TiO<sub>2</sub>-coated cotton fabrics with a dye concentration of 0.16, 0.08, 0.016 and 0.01 mg/L, respectively.

The proposed mechanism for the visible-light-driven, photo-catalytic activity of TiO<sub>2</sub> in the presence of the dye sensitizer is explained in Figure 7. When dye sensitizer is exposed to a visible light source with sufficient light intensity, the electrons are excited from highest occupied molecular orbital (HOMO) of the dye to the lowest unoccupied molecular orbital (LUMO), from which electrons jumps to the conduction band of the TiO<sub>2</sub>. Thus, an increase in the electron density in the conduction band of the TiO<sub>2</sub> increases its photo-catalytic activity under visible light [21].

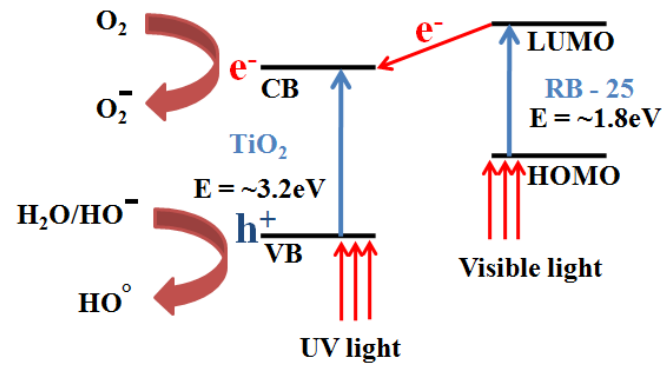


**Figure 7.** Schematic diagram of mechanism of dye-sensitized TiO<sub>2</sub> acting as a photo-catalyst.

### 3.4. Color Yield Measurements

The *K/S* sum values obtained from the reflectance spectrophotometer (Macbeth Color-Eye 7000A) of all the test specimens are given in Table 3. The results show that with the increasing sensitizer dye concentration of the TiO<sub>2</sub>-coated cotton fabric, the *K/S* sum value increases, resulting in more color yield. However, the color yield was reduced to some extent when the samples were irradiated for 6 h, as shown in Figure 8.

**Table 3.** *K/S* sum values and CIE color coordinates values of the test samples.

Description of the Fabric Specimen		<i>K/S</i> Sum Value	<i>L</i> *	<i>a</i> *	<i>b</i> *
<i>Before irradiation</i>					
1	With dye concentration of 0.01 mg/L	5.107	81.998	−8.86	0.079
2	With dye concentration of 0.016 mg/L	5.628	81.388	−10.923	−1.162
3	With dye concentration of 0.08 mg/L	6.421	80.633	−12.353	−3.395
4	With dye concentration of 0.16 mg/L	11.687	76.343	−18.238	−7.898
<i>After irradiation</i>					
5	With dye concentration of 0.01 mg/L	4.776	82.75	−7.503	−1.125
6	With dye concentration of 0.016 mg/L	5.442	82.085	−9.35	−1.734
7	With dye concentration of 0.08 mg/L	6.098	81.065	−10.577	−4.077
8	With dye concentration of 0.16 mg/L	10.455	77.291	−17.26	−8.604
<i>Specimens with stains before irradiation</i>					
9	With dye concentration of 0.01 mg/L	5.535	81.464	1.651	0.848
10	With dye concentration of 0.016 mg/L	6.078	80.71	−2.778	−1.237
11	With dye concentration of 0.08 mg/L	6.832	78.974	−3.222	−4.274
12	With dye concentration of 0.16 mg/L	11.798	73.494	−6.635	−8.712
<i>Specimens with stains after irradiation</i>					
13	With dye concentration of 0.01 mg/L	4.852	81.969	−1.233	−0.46
14	With dye concentration of 0.016 mg/L	5.593	81.541	−3.753	−2.383
15	With dye concentration of 0.08 mg/L	6.348	79.845	−2.872	−4.412
16	With dye concentration of 0.16 mg/L	11.509	74.248	−6.621	−8.95



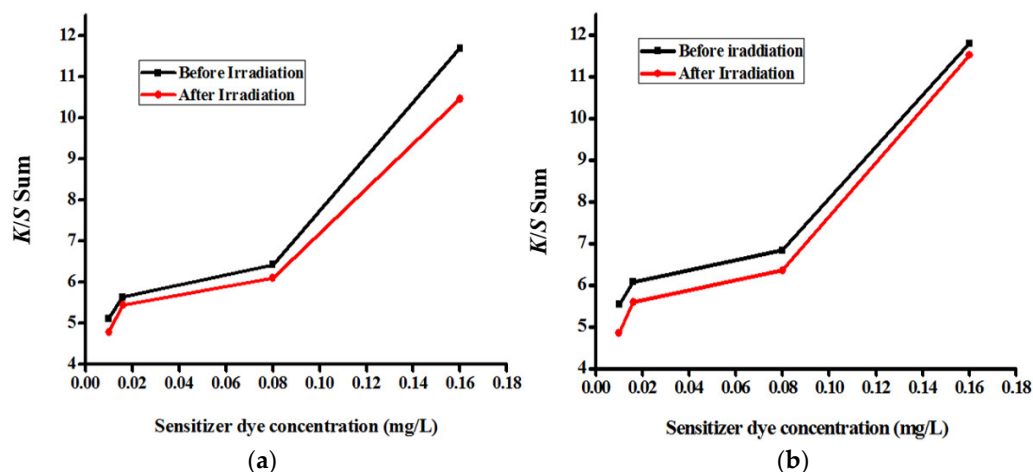


**Figure 8.**  $K/S$  sum values against sensitizer dye concentration: (a) Only RB-25 dye and (b) RB-25 dye with RhB stain.

### 3.5. CIE Color Coordinates

The CIE color coordinate values of all the samples are given in Table 3. The  $L^*$  values of dye/ $\text{TiO}_2$ -coated cotton fabrics decreased with an increase in the dye concentration of the sensitizer. Also, it is noted that the  $L^*$  value decreased when stains were applied to the dye/ $\text{TiO}_2$ -coated cotton fabrics. However, with irradiation, the  $L^*$  value increased, which indicates degradation of the dye attached to the  $\text{TiO}_2$  surface, as shown in Figure 9. This pattern of change in  $L^*$  values agrees with the  $K/S$  sum values of the same samples.

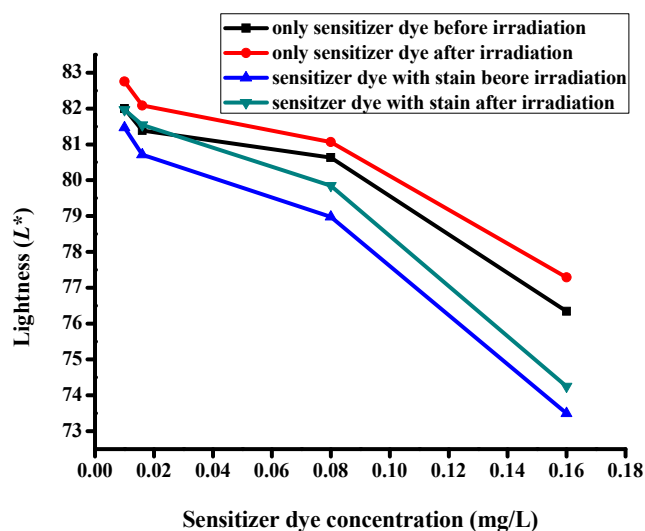


**Figure 9.** The  $L^*$  values of dye/ $\text{TiO}_2$ -coated cotton fabric.

The  $a^*$  value is associated with the redness and greenness of the test specimen. The greater value of  $a^*$  corresponds to the reddish shade of the sample. Figure 10 represents the  $a^*$  values of dye/ $\text{TiO}_2$ -coated cotton fabrics with and without stains of RhB. The figure shows that the  $a^*$  value increased significantly when the RhB dye stain was applied to the  $\text{TiO}_2$ /dye-coated fabrics. This increase in  $a^*$  value is the result of the reddish color of the RhB stain. However, the  $a^*$  value decreased when irradiated with the visible light. This decrease is significant in only those samples which have a lower concentration of the sensitizer dye, which proves the agreement of the RhB degradation, as explained in Section 3.3.

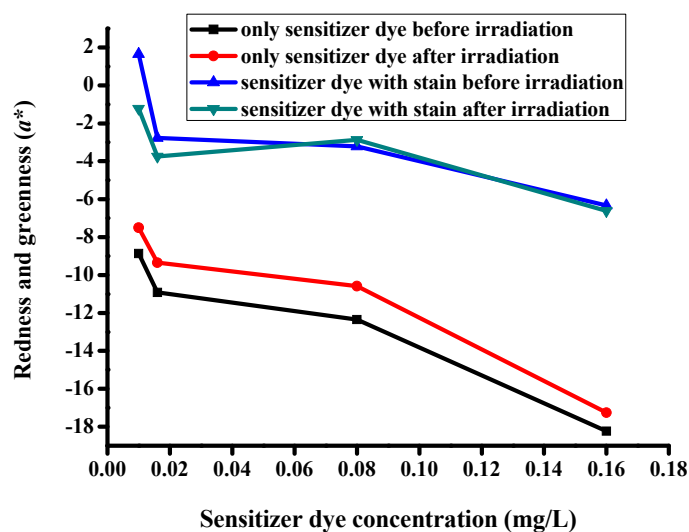


Figure 10. The  $a^*$  values of the dye/TiO<sub>2</sub>-coated cotton fabrics.

The value of  $b^*$  represents the blueness and yellowness of the test samples. The basic principle for the yellowish and bluish appearance of the samples is that the greater the value of  $b^*$ , the more yellowish its appearance [33]. The plot of the  $b^*$  values of the dye/TiO<sub>2</sub>-coated samples before and after irradiation are given in Figure 11. It is apparent from the plots that the blueness of the samples increases as the sensitizer dye concentration is increased on the cotton fabric samples, which are in accordance with the  $K/S$  values. The  $b^*$  value is increased when the stain is applied to the cotton fabric with the lowest sensitizer concentration, as indicated in the blue plot in Figure 11. This might be due to the basic color of the RhB that is more apparent when the sensitizer dye concentration is low. When the sensitizer dye concentration is increased, the  $b^*$  value decreases, which indicates that the yellowish appearance of the stain is less prominent as the bluish color dominates with the increasing dye concentration, due to the inherent blue color of the sensitizer dye. After irradiation, the  $b^*$  value decreased significantly for the stained sample, which had lowest sensitizer dye concentration, as shown in the green plot of Figure 11. This is due to the fact that the photo-catalytic efficiency of the samples is greater at the lower sensitizer dye concentration.

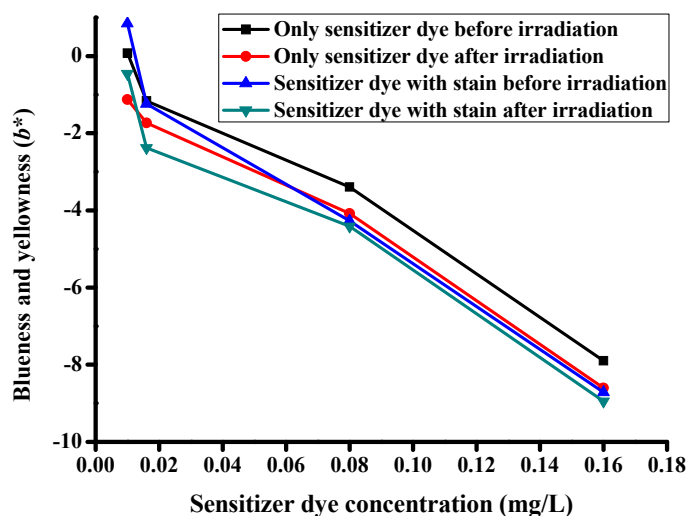
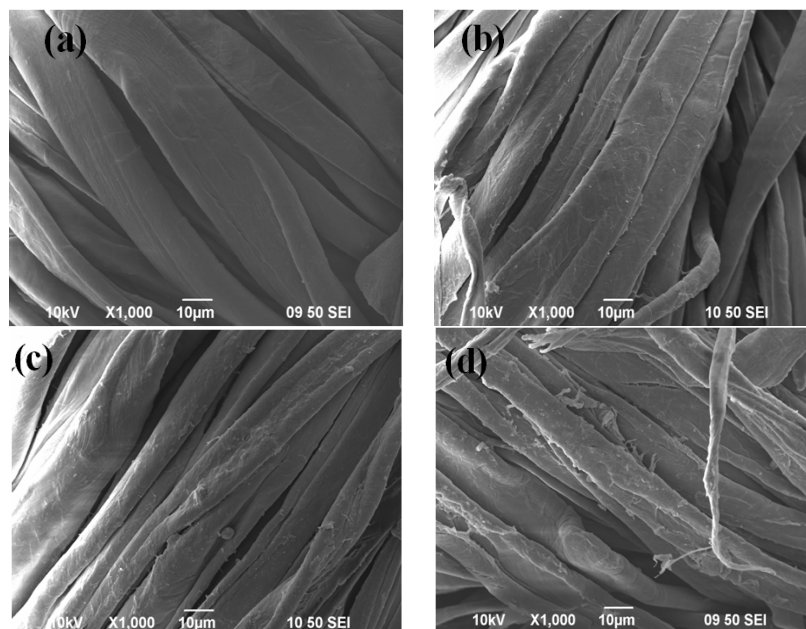


Figure 11. The  $b^*$  values of dye/TiO<sub>2</sub>-coated cotton fabrics.

### 3.6. Surface Morphology

The scanning electron microscope (SEM) images of the pure cotton, TiO<sub>2</sub> coated and dye/TiO<sub>2</sub>-coated cotton fabrics are given in the Figure 12.



**Figure 12.** SEM Images of (a) pure cotton fabric, (b) TiO<sub>2</sub> coated cotton fabric, (c) dye/TiO<sub>2</sub> coated cotton fabric and (d) dye/TiO<sub>2</sub> coated cotton fabric with high concentration of RB-25.

The rough surface as shown in Figure 12b shows that TiO<sub>2</sub> nano-particles have been successfully coated on the cotton fabric. The dye molecules of RB-25 present of the can also be seen in the images in Figure 12c,d. However, it can be seen that when the concentration of dye increased, the dye molecules started to agglomerate at the surface, as shown in Figure 12d.

### 3.7. Stain Degradation on Fabrics during Self-Cleaning Test

The images of stain degradation on fabrics during the self-cleaning test are shown in Figure 13. It is clear from the figure that stains of RhB were removed after 6 h of irradiation. The efficiency of self-cleaning increased with decreasing dye concentrations on the TiO<sub>2</sub>-coated cotton fabric.

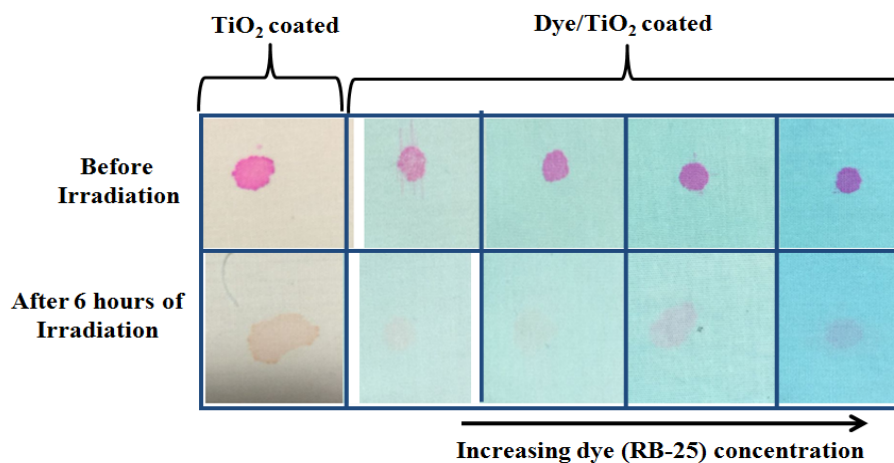


**Figure 13.** The images of stain degradation on fabrics during the self-cleaning test.

#### 4. Conclusions

In this study, visible-light-driven, self-cleaning cotton fabrics were developed by coating the cotton fabric with dye-sensitized TiO<sub>2</sub>. A PC-based reactive dye (RB-25) was used as a dye-sensitizer for TiO<sub>2</sub>. TiO<sub>2</sub> nano-sol was prepared via the sol-gel method, and this TiO<sub>2</sub> nano-sol was coated on the cotton fabric by the dip-pad-dry-cure method. The TiO<sub>2</sub>-coated cotton fabric was then dyed with reactive Blue-25. The photo-catalytic self-cleaning efficiency of the resulting dye/TiO<sub>2</sub>-coated cotton fabrics was evaluated by the degradation of RhB and color co-ordinate measurements. The Dye/TiO<sub>2</sub>-coated cotton fabrics showed good photo-catalytic properties under visible light.

**Acknowledgments:** The project is financially supported by Institute of Textiles and Clothing, The Hong Kong Polytechnic University.

**Author Contributions:** All the research work for this study was conducted by Ishaq Ahmad. The article draft was written by Ishaq Ahmad. Chi-wai Kan supervised and finalized the draft for publication.

**Conflicts of Interest:** The authors declare no conflict of interest.

#### References

1. Horrocks, A.R.; Anand, S.C. *Handbook of Technical Textiles*; Elsevier: Amsterdam, The Netherlands, 2000.
2. Ahmad, I.; Kan, C.-W. A review on development and applications of bio-inspired super-hydrophobic textiles. *Materials* **2016**, *9*, 892. [[CrossRef](#)] [[PubMed](#)]
3. Barthlott, W.; Neinhuis, C. Purity of the sacred lotus, or escape from contamination in biological surfaces. *Planta* **1997**, *202*, 1–8. [[CrossRef](#)]
4. Cai, P.; Zhou, S.-M.; Ma, D.-K.; Liu, S.-N.; Chen, W.; Huang, S.-M. Fe<sub>2</sub>O<sub>3</sub>-modified porous BiVO<sub>4</sub> nanoplates with enhanced photo-catalytic activity. *Nano-Micro Lett.* **2015**, *7*, 183–193. [[CrossRef](#)]
5. Dotan, H.; Sivula, K.; Grätzel, M.; Rothschild, A.; Warren, S.C. Probing the photo-electrochemical properties of hematite ( $\alpha$ -Fe<sub>2</sub>O<sub>3</sub>) electrodes using hydrogen peroxide as a hole scavenger. *Energy Environ. Sci.* **2011**, *4*, 958–964. [[CrossRef](#)]
6. Ashraf, M.; Champagne, P.; Perwuelz, A.; Campagne, C.; Leriche, A. Photo-catalytic solution discoloration and self-cleaning by polyester fabric functionalized with ZnO nanorods. *J. Ind. Text.* **2015**, *44*, 884–898. [[CrossRef](#)]
7. Ofori, F.A.; Sheikh, F.A.; Appiah-Ntiamoah, R.; Yang, X.; Kim, H. A simple method of electrospun tungsten trioxide nanofibers with enhanced visible-light photo-catalytic activity. *Nano-Micro Lett.* **2015**, *7*, 291–297. [[CrossRef](#)]
8. Qi, K.; Daoud, W.A.; Xin, J.H.; Mak, C.L.; Tang, W.; Cheung, W. Self-cleaning cotton. *J. Mater. Chem.* **2006**, *16*, 4567–4574. [[CrossRef](#)]
9. Fujishima, A.; Zhang, X.; Tryk, D.A. TiO<sub>2</sub> photocatalysis and related surface phenomena. *Surf. Sci. Rep.* **2008**, *63*, 515–582. [[CrossRef](#)]
10. Tan, B.; Gao, B.; Guo, J.; Guo, X.; Long, M. A comparison of TiO<sub>2</sub> coated self-cleaning cotton by the sols from peptizing and hydrothermal routes. *Surf. Coat. Technol.* **2013**, *232*, 26–32. [[CrossRef](#)]
11. Grandcolas, M.; Louvet, A.; Keller, N.; Keller, V. Layer-by-layer deposited titanate-based nanotubes for solar photo-catalytic removal of chemical warfare agents from textiles. *Angew. Chem. Int. Ed.* **2009**, *48*, 161–164. [[CrossRef](#)] [[PubMed](#)]
12. Rtimi, S.; Pulgarin, C.; Sanjines, R.; Kiwi, J. Innovative semi-transparent nanocomposite films presenting photo-switchable behavior and leading to a reduction of the risk of infection under sunlight. *RSC Adv.* **2013**, *3*, 16345–16348. [[CrossRef](#)]
13. Baghriche, O.; Rtimi, S.; Pulgarin, C.; Roussel, C.; Kiwi, J. RF-plasma pretreatment of surfaces leading to TiO<sub>2</sub> coatings with improved optical absorption and OH-radical production. *Appl. Catal. B Environ.* **2013**, *130*, 65–72. [[CrossRef](#)]
14. Rtimi, S.; Giannakis, S.; Bensimon, M.; Pulgarin, C.; Sanjines, R.; Kiwi, J. Supported TiO<sub>2</sub> films deposited at different energies: Implications of the surface compactness on the catalytic kinetics. *Appl. Catal. B Environ.* **2016**, *191*, 42–52. [[CrossRef](#)]

15. Wu, D.; Long, M. Low-temperature synthesis of N-TiO<sub>2</sub> sol and characterization of N-TiO<sub>2</sub> coating on cotton fabrics. *Surf. Coat. Technol.* **2012**, *206*, 3196–3200. [[CrossRef](#)]
16. Uddin, M.; Cesano, F.; Scarano, D.; Bonino, F.; Agostini, G.; Spoto, G.; Bordiga, S.; Zecchina, A. Cotton textile fibres coated by Au/TiO<sub>2</sub> films: Synthesis, characterization and self-cleaning properties. *J. Photochem. Photobiol. A Chem.* **2008**, *199*, 64–72. [[CrossRef](#)]
17. Yuranova, T.; Rincon, A.; Pulgarin, C.; Laub, D.; Xantopoulos, N.; Mathieu, H.-J.; Kiwi, J. Performance and characterization of Ag-cotton and Ag/TiO<sub>2</sub> loaded textiles during the abatement of *E. coli*. *J. Photochem. Photobiol. A Chem.* **2006**, *181*, 363–369. [[CrossRef](#)]
18. Pakdel, E.; Daoud, W.A.; Sun, L.; Wang, X. Visible and UV functionality of TiO<sub>2</sub> ternary nanocomposites on cotton. *Appl. Surf. Sci.* **2014**, *321*, 447–456. [[CrossRef](#)]
19. Pakdel, E.; Daoud, W.A.; Wang, X. Self-cleaning and super-hydrophilic wool by TiO<sub>2</sub>/SiO<sub>2</sub> nanocomposite. *Appl. Surf. Sci.* **2013**, *275*, 397–402. [[CrossRef](#)]
20. Afzal, S.; Daoud, W.A.; Langford, S.J. Self-cleanin cotton by porphyrin-sensitized visible-light photo-catalysis. *J. Mater. Chem.* **2012**, *22*, 4083–4088. [[CrossRef](#)]
21. Afzal, S.; Daoud, W.A.; Langford, S.J. Photostable self-cleaning cotton by a copper(II) porphyrin/TiO<sub>2</sub> visible-light photo-catalytic system. *ACS Appl. Mater. Interfaces* **2013**, *5*, 4753–4759. [[CrossRef](#)] [[PubMed](#)]
22. Afzal, S.; Daoud, W.A.; Langford, S.J. Visible-light self-cleaning cotton by metalloporphyrin-sensitized photo-catalysis. *Appl. Surf. Sci.* **2013**, *275*, 36–42. [[CrossRef](#)]
23. Afzal, S.; Daoud, W.A.; Langford, S.J. Super-hydrophobic and photo-catalytic self-cleaning cotton. *J. Mater. Chem. A* **2014**, *2*, 18005–18011. [[CrossRef](#)]
24. Sakamoto, K.; Ohno-Okumura, E. Syntheses and functional properties of phthalocyanines. *Materials* **2009**, *2*, 1127–1179. [[CrossRef](#)]
25. Ali, H.; Van Lier, J.E. Metal complexes as photo-and radiosensitizers. *Chem. Rev.* **1999**, *99*, 2379–2450. [[CrossRef](#)] [[PubMed](#)]
26. Marais, E.; Klein, R.; Antunes, E.; Nyokong, T. Photocatalysis of 4-nitrophenol using zinc phthalocyanine complexes. *J. Mol. Catal. A Chem.* **2007**, *261*, 36–42. [[CrossRef](#)]
27. Hu, M.; Xu, Y.; Zhao, J. Efficient photosensitized degradation of 4-chlorophenol over immobilized aluminum tetrasulfophthalocyanine in the presence of hydrogen peroxide. *Langmuir* **2004**, *20*, 6302–6307. [[CrossRef](#)] [[PubMed](#)]
28. Ranjit, K.T.; Willner, I.; Bossmann, S.; Braun, A. Iron(III) phthalocyanine-modified titanium dioxide: A novel photocatalyst for the enhanced photodegradation of organic pollutants. *J. Phys. Chem. B* **1998**, *102*, 9397–9403. [[CrossRef](#)]
29. Kan, C.-W.; Lam, C.-F.; Chan, C.-K.; Ng, S.-P. Using atmospheric pressure plasma treatment for treating grey cotton fabric. *Carbohydr. Polym.* **2014**, *102*, 167–173. [[CrossRef](#)] [[PubMed](#)]
30. Portella, E.H.; Romanzini, D.; Angrizani, C.C.; Amico, S.C.; Zattera, A.J. Influence of stacking sequence on the mechanical and dynamic mechanical properties of cotton/glass fiber reinforced polyester composites. *Mater. Res.* **2016**, *19*, 542–547. [[CrossRef](#)]
31. Giesz, P.; Celichowski, G.; Puchowicz, D.; Kamińska, I.; Grobelny, J.; Batory, D.; Cieślak, M. Microwave-assisted TiO<sub>2</sub>: Anatase formation on cotton and viscose fabric surfaces. *Cellulose* **2016**, *23*, 2143–2159. [[CrossRef](#)]
32. Jain, R.; Mathur, M.; Sikarwar, S.; Mittal, A. Removal of the hazardous dye rhodamine B through photocatalytic and adsorption treatments. *J. Environ. Manag.* **2007**, *85*, 956–964. [[CrossRef](#)] [[PubMed](#)]
33. Kan, C.W.; Yuen, C.W. Effect of atmospheric pressure plasma treatment on the desizing and subsequent colour fading process of cotton denim fabric. *Color. Technol.* **2012**, *128*, 356–363. [[CrossRef](#)]

